A LINEAR INDUCTION MOTOR PARAMETER DETERMINATION METHOD

*Euler B. dos Santos, MSc*** *Luciano Martins Neto,Dr**
*José R. Camacho,PhD** *Ricardo S. T. Pontes,MSc****
*Universidade Federal de Uberlândia, Depto Engenharia Elétrica
UFU / DEENE / LabMaq
P.O.Box: 593 - Campus Santa Mônica
38400-902 - Uberlândia - MG – Brasil
e.mail: jrcamacho@ufu.br
******Universidade Federal de Goiás, Escola de Engenharia Elétrica
74605-020 - Goiânia - GO - Brasil
***Universidade Federal do Ceará, Depto de Engenharia Elétrica
Fortaleza - CE – Brasil

***Abstract* - The main goal in this paper is to present a linear induction motor parameter determination method when its destination is mainly the thrust development. This method is developed basically from the equivalence between the Linear Induction Motor (LIM) and the ordinary asymmetrical induction motor. In this case it is used the theory of symmetrical and asymmetrical components of positive, negative and zero sequence. Experimental procedures with the LIM prototype can support the theoretical and experimental validation for this method.**

I. INTRODUCTION

The purpose of this work is to develop a methodology to obtain the parameters based on the symmetrical components theory. It is observed the unbalanced phase current and voltages, with a theoretical and experimental validation. In this case it is possible to imagine an ordinary but asymmetrical induction motor which has the characteristics equivalent to the mentioned LIM. Following this philosophy, the whole model is made considering the ordinary asymmetrical induction motor. The asymmetry in question can be any, for example: the different number of turns in each phase of the stator and rotor, different resistance and reactance in each phase, etc.

II. PROTOTYPE

In this work, a three-phase, two pole, two-sided with short primary LIM, was built and tested in the Electrical Machines Laboratory. The primary stacks (stator) are made of steel silicon sheets (core) and the secondary (linor) constituted of a non-ferromagnetic material, the aluminum, with the shape of a flat disc, which illustrated in Figure 1.

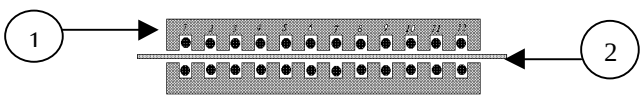

Figure 1 – Linear induction motor: 1 – primary package, 2 – secondary in an aluminum disc.

The primary winding in each stack is made of copper, three-phase, concentric type, set of steps 1:8 and 2:7, one layer, 200 turns in each phase with coil scheme shown in Figure 2.

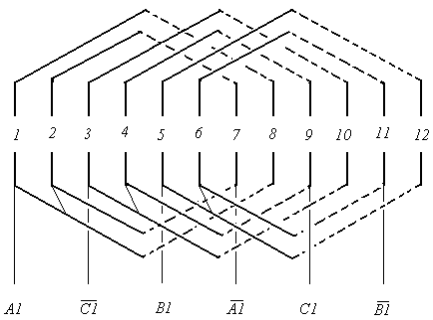

Figure 2 – Winding scheme for each primary package.

The architecture of primary packages has finite length, the primary winding is spread along the direction of movement, the secondary structure is a solid aluminum disc. The relative movement between primary and secondary is the cause of interesting phenomena called *border effects*, and also the unbalance in phase voltage and currents. Border effects are mainly caused by the opened structure of a LIM, regarding its magnetic circuit, when compared with the closed structure of an ordinary three-phase induction motor[4].

III. MATHEMATICAL MODEL

The asymmetrical induction motor, in order to make the equations clearer, will be considered with a different number of turns per phase N_a, N_b and N_c.

A LIM when fed by a sinusoidal three-phase balanced line voltage system presents in its terminal currents and voltages which are not balanced. This happens due to the design aspects and border effects.

The voltage equation in a primary generic phase k (*a*, *b* or *c*) can be written as follows:

$$\dot{V}_k = \dot{Z}_k \ \dot{I}_k + \dot{E}_k \qquad (1)$$

where:

$\dot{V}_k$ - voltage vector in a generic primary phase k;

$\dot{Z}_k$ - impedance, a representation of primary winding leakage reactance and resistance, for the generic phase k;

$\dot{I}_k$ - current vector for the primary generic phase k;

$\dot{E}_k$ - primary winding electromotrice force(*emf*), for the generic phase k.

Taking into consideration the phase sequence as being ABC and phase A as the reference, the unbalanced feeding current system can be decomposed in its symmetrical components. Knowing that the primary winding is Y connected with floating neutral, the current positive ($\dot{I}_1$) and negative ($\dot{I}_2$) sequence components[2] can be obtained, with the unbalance degree ($\dot{g}_d$) given by:

$$\dot{g}_d = \frac{\dot{I}_2}{\dot{I}_1} \tag{2}$$

The *electromotrice forces* (*emf*) will have positive $\left(\dot{E}_{ap}, \dot{E}_{bp}, \dot{E}_{cp}\right)$ and negative $\left(\dot{E}_{an}, \dot{E}_{bn}, \dot{E}_{cn}\right)$ sequence components. Through Faraday's Law the relationship among these components are given by:

$$b\,\dot{E}_{bp} = \alpha^2 \dot{E}_{ap} \qquad b\,\dot{E}_{bn} = \alpha \dot{E}_{ap} \tag{3}$$

$$c\,\dot{E}_{cp} = \alpha \dot{E}_{ap} \qquad c\,\dot{E}_{cn} = \alpha^2 \dot{E}_{an} \tag{4}$$

with b and c being real numbers and $\alpha = e^{[j(2\pi/3)]}$.

With $\dot{Z}_{ap}$ and $\dot{Z}_{an}$ being the positive and negative sequence impedance, the result of a parallel association of the magnetization reactance with the corresponding secondary sequence impedance. Taking into consideration the *phase A*, the *emf* can be related with currents through equations (5) and (6).

$$\dot{Z}_{ap} = \frac{\dot{E}_{ap}}{\dot{I}_{ap}} \tag{5} \qquad \dot{Z}_{an} = \frac{\dot{E}_{an}}{\dot{I}_{an}} \tag{6}$$

Where $\dot{I}_{ap}$ and $\dot{I}_{an}$ are asymmetric positive and negative sequence components respectively.

With some algebraic manipulation can be obtained:

$$\begin{bmatrix} \dot{V}_a \\ \dot{V}_b \\ \dot{V}_c \end{bmatrix} = \begin{bmatrix} \dot{Z}_a(1+g_d) & \dot{Z}_{ap} & \dot{Z}_{an} \\ \dot{Z}_b(\alpha^2+\alpha g_d) & \dot{Z}_{ap}\dfrac{\alpha^2}{b} & \dot{Z}_{an}\dfrac{\alpha}{b} \\ \dot{Z}_c(\alpha+\alpha^2 g_d) & \dot{Z}_{ap}\dfrac{\alpha}{c} & \dot{Z}_{an}\dfrac{\alpha^2}{c} \end{bmatrix} \begin{bmatrix} \dot{I}_1 \\ \dot{I}_{ap} \\ \dot{I}_{an} \end{bmatrix} \tag{7}$$

The developed positive (F_p), negative (F_n) sequence and resulting (FR) thrust are given by:

$$F_p = 3\Re_e\left[\dot{I}^*_{ap}.\dot{E}_{ap}\right] . \left(\frac{1}{v_{sx}}\right) \tag{8}$$

$$F_n = -3\Re_e\left[\dot{I}^*_{an}.\dot{E}_{an}\right] . \left(\frac{1}{v_{sx}}\right) \tag{9}$$

$$F_R = F_p + F_n \tag{10}$$

with v_{sx} being the linear synchronous speed.

IV. TESTS AND EXPERIMENTAL RESULTS

The first step to obtain the LIM parameters is to get experimentally the leakage inductance following the procedures from reference [1].

The primary phase resistance is obtained through direct measurements. The magnetization reactance is obtained from no-load tests; this test can be made without a linor or with a moving linor at synchronous linear speed.

Determination of secondary impedance is made with a locked linor. In both cases the experimental procedure follow the scheme in Figure 3.

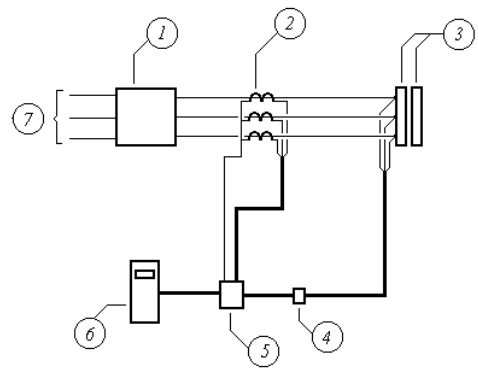

Specifications:

(1) AC Power Source /analyzer
Frequency: 45/1000 Hz;
Voltage: 0 – 300V;
Power: 4,5 KVA;
(2) Current Hall effect sensor;
(3) Set of two blocks defining the stator;
(4) Voltage Hall effect sensor;
(5) Data acquisition system;
(6) Personal Computer CPU;
(7) Feeding from the mains.

Figure 3 - Laboratory scheme to obtain voltage and current waveforms.

The current signal is obtained through the application to the machine of a sinusoidal three-phase balanced voltage system. As an illustration Figures 4, 5 and 6, show the line voltage, phase voltages and current waveforms respectively. Those results were obtained in one of the tests performed. This is a case of locked linor under an applied "*rms*" line voltage of 75.699 V.

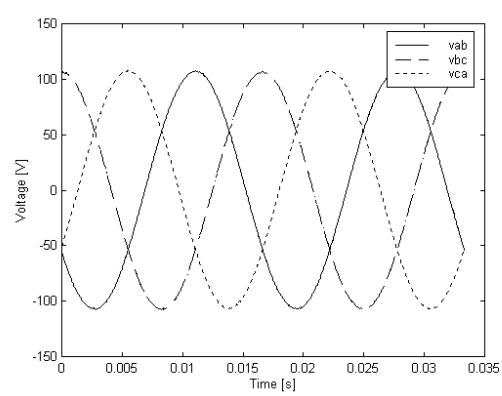

Figure 4 - Line voltages for a locked linor under an applied "*rms*" line voltage of 75.699 V.

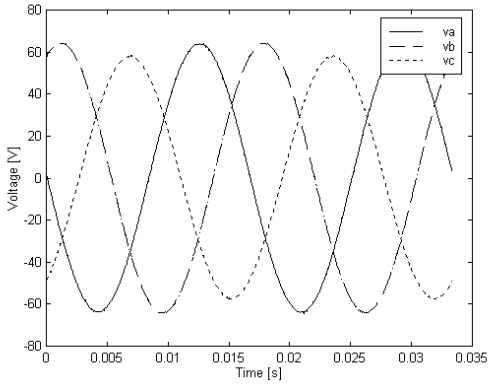

Figure 5 - Phase voltages for a locked linor under the same conditions as in Figure 4.

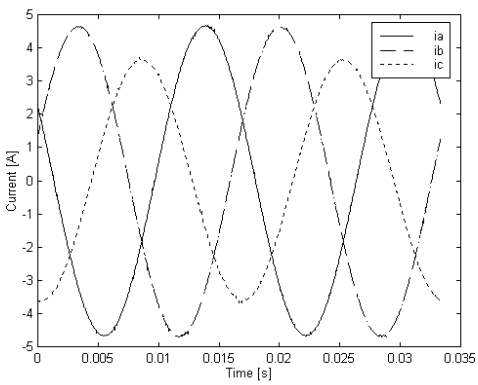

Figure 6 - Phase currents for a locked linor under the same conditions as in Figure 4.

Voltage and current waveforms obtained have time harmonics of high order. Therefore, the use of Fast Fourier Transform (FFT) allow the acquisition of harmonic content magnitude up to a certain order, which in our case, following international standards, is the 50th harmonic. It will be possible then, to obtain the Total Harmonic Distortion (THD). Table 1 shows in percentage values relative to the fundamental component of harmonic contents up to the 7th order. Those values were obtained from phase voltages and currents in Figures 5 and 6.

Table 1 - Percentage values relative to the fundamental component of harmonic content up to the 7th order - From phase voltages and currents in Figures 5 and 6.

-------	V_a	V_b	V_c	I_a	I_b	I_c
Fund	100	100	100	100	100	100
2nd	0.0616	0.0240	0.0470	0.0589	0.0285	0.0332
3rd	0.1680	0.1443	0.0758	0.1042	0.0755	0.0640
4th	0.0868	0.0424	0.0535	0.0458	0.0244	0.0279
5th	0.1004	0.0701	0.1164	0.0288	0.0190	0.0586
6th	0.1288	0.0407	0.0779	0.0467	0.0201	0.0431
7th	0.0141	0.0412	0.0066	0.0296	0.0119	0.0380

A data acquisition system is used to get the feeding voltage and current for each test. Since the THD in time for voltage and current is always lower than 0.5 %. Only first harmonic time components are considered in this case. Therefore, it is obtained, the correspondent complex values for voltage and current waveforms. The mathematical development presented previously allow us to obtain the parameter values.

Table 2 – Values (Ohm) of the experimentally obtained LIM parameters.

IMPEDANCE			MAGNETIZATION REACTANCE
PHASE	PRIMARY	SECONDARY	
A	5.3479 + j5.7290	11.6082 + j1.2342	35.0542

Table 3. Measured (m) currents (A), calculated (c) rms values and percentage difference (diff), against measurements.

Phase A		
Ia (m)	Ia (c)	diff.
1.4084	1.3581	3.5681
2.0252	1.9879	1.8431
2.2292	2.2155	0.6159
2.2888	2.2646	1.0612
2.7115	2.6928	0.6916
2.9109	2.8956	0.5280
3.0914	3.0579	1.0849
3.2980	3.2978	0.0036
3.4243	3.5409	-3.4059

Phase B		
Ib (m)	Ib (c)	diff.
1.4105	1.3558	3.8742
2.0251	1.9845	2.0058
2.2271	2.2117	0.6896
2.2887	2.2607	1.2235
2.7091	2.6882	0.7697
2.9073	2.8907	0.5721
3.0862	3.0527	1.0838
3.2923	3.2923	0.0003
3.4172	3.5349	-3.4448

Phase C		
Ic (m)	Ic (c)	diff.
1.1028	1.0578	4.0804
1.5805	1.5483	2.0370
1.7494	1.7256	0.7902
1.7857	1.7638	1.2231
2.1159	2.0974	0.8760
2.2691	2.2553	0.6086
2.4110	2.3818	1.2129
2.5687	2.5687	0.0016
2.6639	2.7580	-3.5301

No-load data test(rms values):
Feeding at balanced line voltage (V) – V_L = 77.0171
Resulting values:
Phase voltages (V):
V_a = 46,9678, V_b = 46.6967, V_c = 39.9741
Phase currents (A);
I_a = 1.4900, I_b = 1.5297, I_c = 0.9897

Locked rotor data test(rms values):
Feeding at balanced line voltage (V) – V_L = 75.6990
Resulting values:
Phase voltages (V):
V_a = 45,0288, V_b = 45.3695, V_c = 40.7952

Phase currents (A):
$I_a = 3.2980$, $I_b = 3.2923$, $I_c = 2.5687$

The obtained parameters are illustrated in Table 2.

V. THEORETICAL AND EXPERIMENTAL VALIDATION

With a locked linor, the developed thrust and *rms* current will them be measured for different applied *rms* voltage values. With the measured voltage values the current and thrust will be consequently calculated and estimated the percentage difference between measured and calculated values. Table 3 shows the theoretical and experimental validation for the following line voltages: 31, 45, 50, 52, 62, 66, 70, 76 and 81 Volts.

Table 3 show the comparison of values of measured (m), calculated (c) currents, and percentage differences (diff) for the above mentioned voltages.

The following figure shows the measured and calculated thrust against line voltage with locked linor.

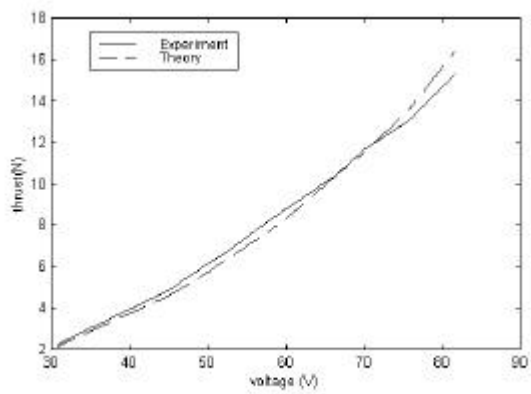

Figure 7 – Thrust against line voltage – linor locked condition.

Table 4 - Measured (m) and calculated (c) thrust values (N), percentage difference (diff) and linear speed (v_x m/s).

THRST (N) MEASURED (m), CALCULATED (c) AND PERCENTAGE DIFERENCE (diff), AGAINST MEASUREMENTS AND LINEAR SPEED v_x (m/s).			
Fp(m)	Fp(c)	diff.	v_x
3.0138	2.4916	17.3287	6.9297
3.3376	2.6762	19.8158	6.7407
3.5890	2.9172	18.7188	6.5122
3.9503	3.2080	18.7908	6.2440
4.4960	3.6402	19.0359	5.7930
6.0354	4.9867	17.3767	4.4948
7.3282	6.7769	7.5220	2.9255
7.6364	7.3752	3.4204	2.2520

This investigation allowed us to measure the thrust against the linear speed, for different operating conditions. To make this measurement a direct current generator was connected to the axis of the secondary disc, with the generator feeding a bank of resistive loads. To achieve a reasonable accuracy in speed measurements a micro processed encoder with an active optical sensor was used. The theoretical and experimental results are presented in Figure 7 and Table 4, showing that the method is reasonably accurate for low speed operation.

Figure 7 and Table 4 shows also how close are the measured and calculated thrust values for different voltages and speeds.

VI. CONCLUSION

The idea of equivalence proved to be a good choice and also can be a tool to make easier future dynamic studies for the linear induction motor. With the given current tables it is easy to verify that the small percentage difference between measured and calculated current values validates the model.

LIM current unbalance is caused not only by its architecture, but also by border effects. In the case of thrust with a moving linear motor, we can easily conclude that the presented model has been validated in low speed conditions. For speed values around 3 m/s as can be seen in Table 4. This table shows the thrust developed against speed.

This work shows a method to obtain LIM phase parameters through the process of obtaining voltage and currents at the machine terminals, when the machine's purpose is thrust development. Therefore the determination of LIM phase parameters becomes possible through experimental tests. So, won't be necessary a large number of restrictive hypothesis when obtaining all this data through theoretical parameter estimation.

In this work were not considered space harmonics, however the method is totally adaptable. More recently obtained results include this effect. They were, obviously, better than the ones presented here, concerning the difference between measured and calculated values of thrust development against speed as shown in Table 4.

VI. REFERENCES

[1] MARTINS NETO, L. e SANTOS, E.B. (1998), Linear Induction Motor Inductance Determination Method - (In Portuguese) - XII CBA, Uberlândia, MG, Brazil.

[2] STEVENSON JR., W. D., (1982), Elements of Power System Analysis, Fourth Edition, McGraw-Hill, New York.

[3] GIERAS, J.F. (1994), Linear Induction Drivers, Clarendon Press, Oxford.

[4] YAMAMURA, S. (1978), Theory of Linear Induction Motors, University of Tokyo Press.

[5] BOLDEA I. and NASAR S. A. (1985), Linear Motion Electromagnetic Systems, John Wiley & Sons, New York.

[6] SIMONE, G. A. (1992), Double Face Linear Asynchronous Converters - Theory and Design, Doctoral Thesis (In Portuguese), FEE – UNICAMP, Campinas, SP, Brazil.

[7] MARTINS NETO, L. (1980), Asymmetrical Three-Phase Induction Motor Phase Number Converter, Doctoral Thesis (In Portuguese), USP - São Carlos, Brazil.